Advancing SOL simulations: avoiding the Boussinesq approximation and coupling closed and open magnetic flux surfaces

J. Morales, B. Frei, F. Halpern, F. Musil, P. Paruta, P. Ricci, F. Riva, M. Siffert and C. Wersal

École Polytechnique Fédérale de Lausanne (EPFL), Swiss Plasma Center (SPC), CH-1015 Lausanne, Switzerland

Why this study?

Plasma turbulence in the SOL and across the last closed flux surface determine the heat load on the walls and the plasma confinement, two crucial issues on the way towards a fusion reactor

What do we present in this poster?

1. A **new formulation of the vorticity equation** that allow us to **relax the Boussinesq approximation**
2. The **energy conservation properties** of the new system of equations
3. **Results of turbulent simulations in the SOL** with and without the Boussinesq approximation with the GBS code [Ricci 2012, Halpern 2016]
4. **Results of turbulent simulations across the last closed flux surface** with the Boussinesq approximation taking into account a cold and a hot ion regime

1. Relaxation of the Boussinesq approximation: new formulation of the vorticity equation

- **Context:** in the Edge-SOL is reasonable to use a fluid approximation, in particular the drift-reduced Braginskii equations [Braginskii 1965, Zeiler 1999]
- **The Boussinesq approximation** is used in the evaluation of the divergence of the polarisation current:

$$\nabla_\perp \cdot \left[\frac{nc}{B\omega_{ci}}\frac{d}{dt}\left(\boldsymbol{E}_\perp - \frac{\nabla_\perp P_i}{en}\right)\right] \approx \frac{nc}{B\omega_{ci}}\frac{d}{dt}\left(\nabla_\perp \cdot \boldsymbol{E}_\perp - \frac{1}{e}\nabla_\perp^2 T_i\right) \quad (1)$$

- **It simplifies the solution of the Poisson equation necessary to evaluate the electric potential**

Derivation of a new vorticity equation

1. We **start** from the **ion momentum equation** given in [Braginskii 1965] – with $\frac{d}{dt} \equiv \frac{\partial}{\partial t} + (\boldsymbol{v}_i \cdot \nabla)$ –

$$m_i\frac{d}{dt}(n\boldsymbol{v}_i) + m_i(n\boldsymbol{v}_i)(\nabla \cdot \boldsymbol{v}_i) = -\nabla P_i - \nabla \cdot \overline{\overline{\Pi}}_i + Zen\left(\boldsymbol{E} + \frac{1}{c}(\boldsymbol{v}_i \times \boldsymbol{B})\right) - \boldsymbol{R}_i, \quad (2)$$

2. **Hypothesis 1:** $\partial/\partial t \approx (\rho_i^2/L_\perp^2)\,\omega_{ci} \ll \omega_{ci}$. Making use of this ordering and taking the cross product of Eq. (2) with the unit vector $\boldsymbol{b} \Longrightarrow$

$$\boldsymbol{v}_{\perp i0} = \boldsymbol{v}_E + \boldsymbol{v}_{di} = c\frac{\boldsymbol{B}\times\nabla\phi}{B^2} + c\frac{\boldsymbol{B}\times\nabla P_i}{ZenB^2}, \quad \text{with } \phi \text{ the electric potential } (\boldsymbol{E} = -\nabla\phi)$$

3. **Hypothesis 2: magnetic field variation on length scales of order R (tokamak major radius), which is larger compared to the perpendicular turbulent length scale** ($L_\perp/R \ll 1$), this implies: $\overline{\overline{\Pi}}_{FLR,0} = -m_i n(\boldsymbol{v}_{di}\cdot\nabla)\,\boldsymbol{v}_i \Longrightarrow$ **'gyro-viscous' cancellation**
4. **Hypothesis 3: plasma quasi-neutrality** ($n = n_e = n_i$). Or, equivalently, we consider the stationary charge conservation equation, $\nabla \cdot \boldsymbol{j} = 0 \Longrightarrow$

$$\nabla \cdot \left(n\boldsymbol{v}_{pol0}\right) + \nabla_\parallel\left(\frac{j_\parallel}{e}\right) + \nabla \cdot (n(\boldsymbol{v}_{di} - \boldsymbol{v}_{de})) = 0 \quad (3)$$

5. **From Eqs. (3), the new formulation of the vorticity equation is:**

$$\frac{\partial\Omega}{\partial t} = -\frac{c}{B}\nabla\cdot\left\{[\phi,\,\omega]\right\} - \nabla\cdot\left\{\nabla_\parallel\left(v_{\parallel i}\omega\right)\right\} + \omega_{ci}\nabla_\parallel\left(\frac{j_\parallel}{e}\right) + \omega_{ci}\nabla\cdot(n(\boldsymbol{v}_{di} - \boldsymbol{v}_{de})) + \frac{1}{3m_i\omega_{ci}}\frac{B}{2}\left(\nabla\times\left(\frac{\boldsymbol{b}}{B}\right)\right)\cdot\nabla G_0 \quad (4)$$

with Ω **the new scalar vorticity:** $\Omega = \nabla\cdot\boldsymbol{\omega} = -\nabla\cdot[\boldsymbol{b}\times(n\boldsymbol{v}_{\perp i0})] = \nabla\cdot(\frac{cn}{B}\nabla_\perp\phi + \frac{c}{ZeB}\nabla_\perp P_i)$ and ω the perpendicular vector: $\boldsymbol{\omega} = -\boldsymbol{b}\times(n\boldsymbol{v}_{\perp i0}) = \frac{cn}{B}\nabla_\perp\phi + \frac{c}{ZeB}\nabla_\perp P_i$.

6. **The Poisson equation for the electric potential** ϕ, $\nabla\cdot(\frac{cn}{B}\nabla_\perp\phi) = \Omega - \frac{c}{ZeB}\nabla_\perp^2 P_i$, is solved with an efficient parallel multigrid method.

2. Energy conservation with the new vorticity equation

- Taking into account the continuity, parallel and temperature equations (for ions and electrons) together with the vorticity equation (4) we obtain the expression of the time evolution of the total energy of the system:

$$\frac{d}{dt}\left\{\int dV\left[\frac{nm_i}{2}\left(v_{\perp i0}^2 + v_{\parallel i}^2\right) + \frac{nm_e}{2}\left(\frac{j_\parallel}{en}\right)^2 + \frac{3}{2}(p_i + p_e) + \frac{1}{8\pi}(\nabla_\perp\psi)^2\right]\right\} = -\int dV\left[\frac{j_\parallel^2}{\sigma_\parallel} + \frac{G_0^2}{3\eta_0}\right] + \varepsilon \quad (5)$$

with

$$\varepsilon = \int dV\left[m_i v_{\perp i0}^2\left(\frac{c}{2Ze}\nabla p_i + cn\nabla\phi\right)\right]\cdot\left\{\nabla\times\frac{\boldsymbol{b}}{B}\right\} + \int dV\left[\frac{mm_i}{2}\boldsymbol{v}_{pol}\cdot\nabla\left(v_{\perp i0}^2 + v_{\parallel i}^2\right) + \frac{3}{2}\boldsymbol{v}_{pol}\cdot\nabla p_i\right]. \quad (6)$$

What do we learn from these equations?

1. The total energy varies because: **Joule, viscous dissipation** and the **approximation made in the drift reduction** of the Braginskii equations (see the ε term Eq. (6))
2. The first term of Eq. (6) is a **curvature term**. **Using Hypothesis 2** we find that this term is smaller than the first term on the left hand side of Eq. (5) by a factor $L_\perp/R \ll 1$
3. The second term of Eq. (6) is of order $(\boldsymbol{v}_{pol}\cdot\nabla)$. Comparing this last term with the corresponding term on the left hand side of Eq. (5), (d/dt), **using Hypothesis 1**: $\boldsymbol{v}_{pol}\cdot\nabla \approx \frac{\rho_i^2}{L_\perp^2}c_s\frac{1}{L_\perp} \approx \frac{\rho_i^2}{L_\perp^2}\frac{\rho_s\omega_{c_i}}{L_\perp} = \frac{\rho_s}{L_\perp}\frac{d}{dt} \ll \frac{d}{dt}$
4. **Therefore, if the dissipation terms can be neglected, the new model conserves the total energy within the ordering used for its deduction**

3. Boussinesq approximation effect in the SOL

- Turbulent simulations in the SOL, taking into account the Boussinesq (*B*) and the non-Boussinesq (*NB*) model
- A safety factor q scan
- We considered cold ions ($\tau = T_{i0}/T_{e0} = 0$) and a hot ion regime ($\tau = 2$)
- **Evaluation of the SOL pressure typical radial length, defined as** $L_P = \left\langle\left|\frac{1}{P}\frac{\partial P}{\partial r}\right|^{-1}\right\rangle$

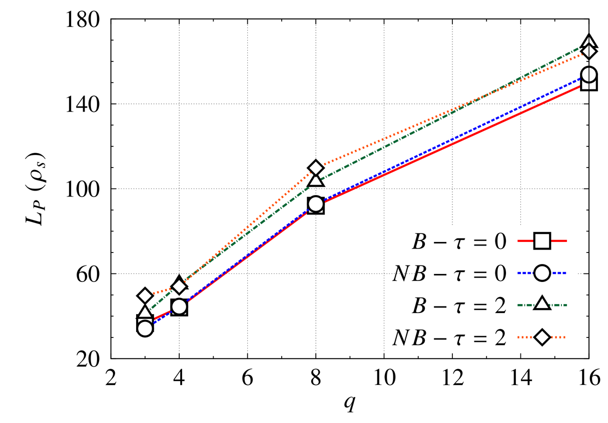

Figure 1: Radial pressure length (ρ_s units) as a function of the safety factor q.

Our findings

1. For $\tau = 0$ the difference in the L_P value between the *B* and the *NB* model is of a few percent (see Fig. 1)
2. **L_P is 10% larger for the *NB* model compared to *B* if $q = 3$ and $\tau = 2$ are considered** (see Fig. 1)

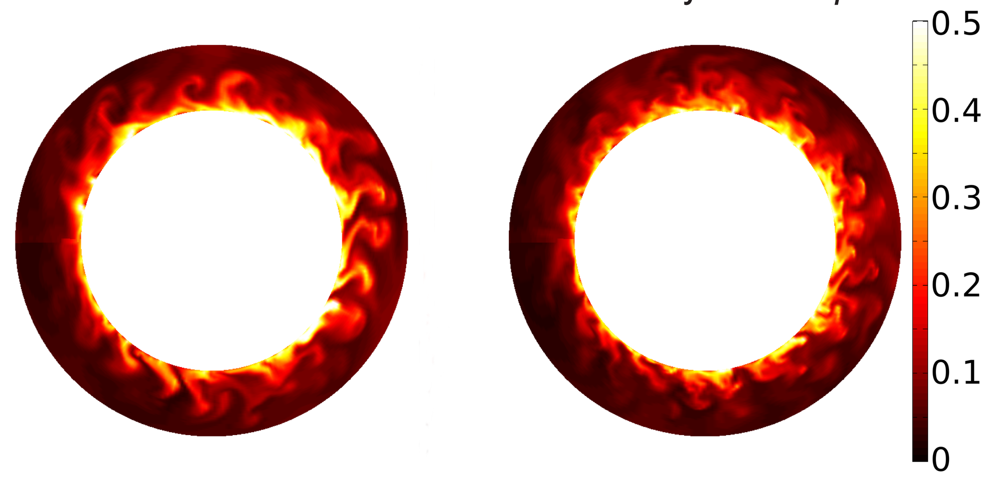

Figure 2: SOL snapshot of the pressure field for *NB* (left) and *B* (right) models, $q = 3$ and $\tau = 2$.

For the case $q = 3$ and $\tau = 2$ (see Figs. 2 and 3):

- **In Fig. 3 –*Left*– a flattening of the pressure profile is visible for the *NB* case**
- **The enhancement of the turbulent transport explains the flattening of P, or increase of L_P**
- In Fig. 3:
  a. For *NB*: the standard deviation has larger values
  b. For *NB*: the pressure spectrum shows stronger fluctuations with lower poloidal mode numbers

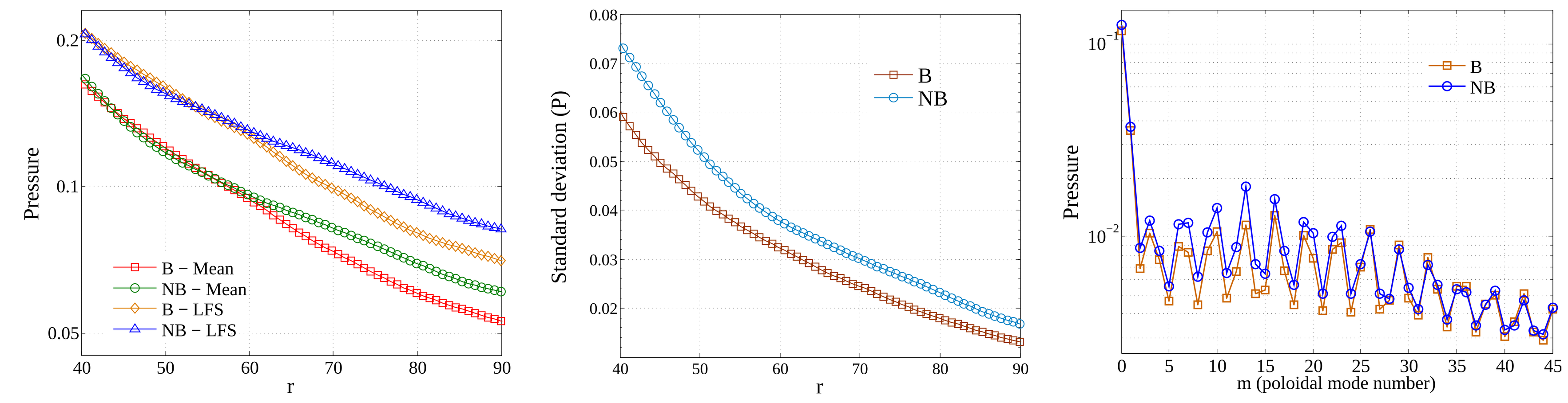

Figure 3: –*Left*– pressure (semi-log), mean profile and profile at the low field side (LFS). –*Center*– standard deviation profile. –*Right*– poloidal mode number spectrum, for $q = 3$ and $\tau = 2$.

4. Averaged plasma profiles at the Last Closed Flux Surface

- Two regimes are considered: $\tau = T_{i0}/T_{e0} = 0$ and a hot ion regime with $\tau = 1$
- The simulations are performed for two normalized resistivities: $\nu = \frac{e^2 n_0 R}{m_i c_s \sigma_\parallel} = \{0.05, 0.1\} \propto n_0 R/T_{e0}^2$
- **We find an increase of the inverse pressure gradient length $|L_P^{-1}|$ at the LCFS for the hot ion case with low resistivity**
- **The increase of $|L_P^{-1}|$ is correlated with the increase of the poloidal $\boldsymbol{E}\times\boldsymbol{B}$ velocity and velocity shear**

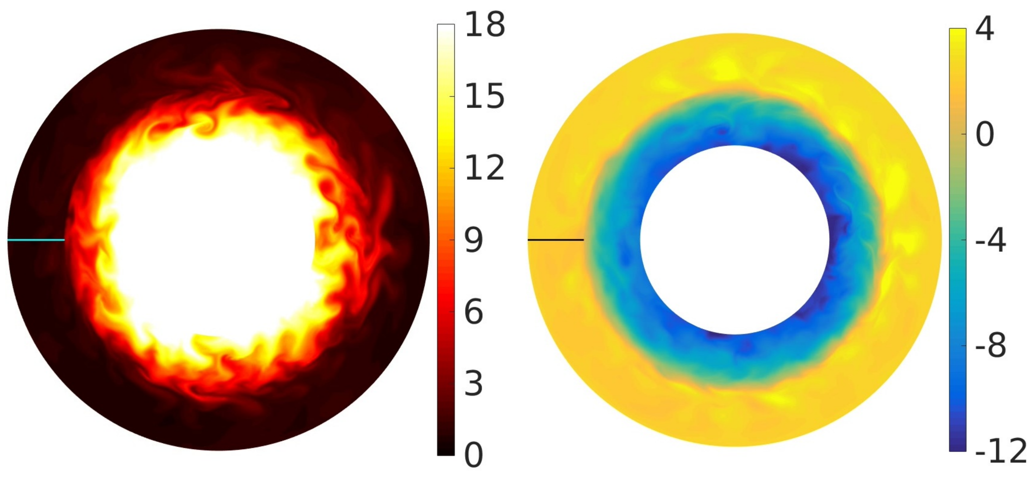

Figure 4: Edge-SOL snapshot of the pressure field –*left*– and electric potential –*right*–, for $\tau = 1$ and $\nu = 0.05$.

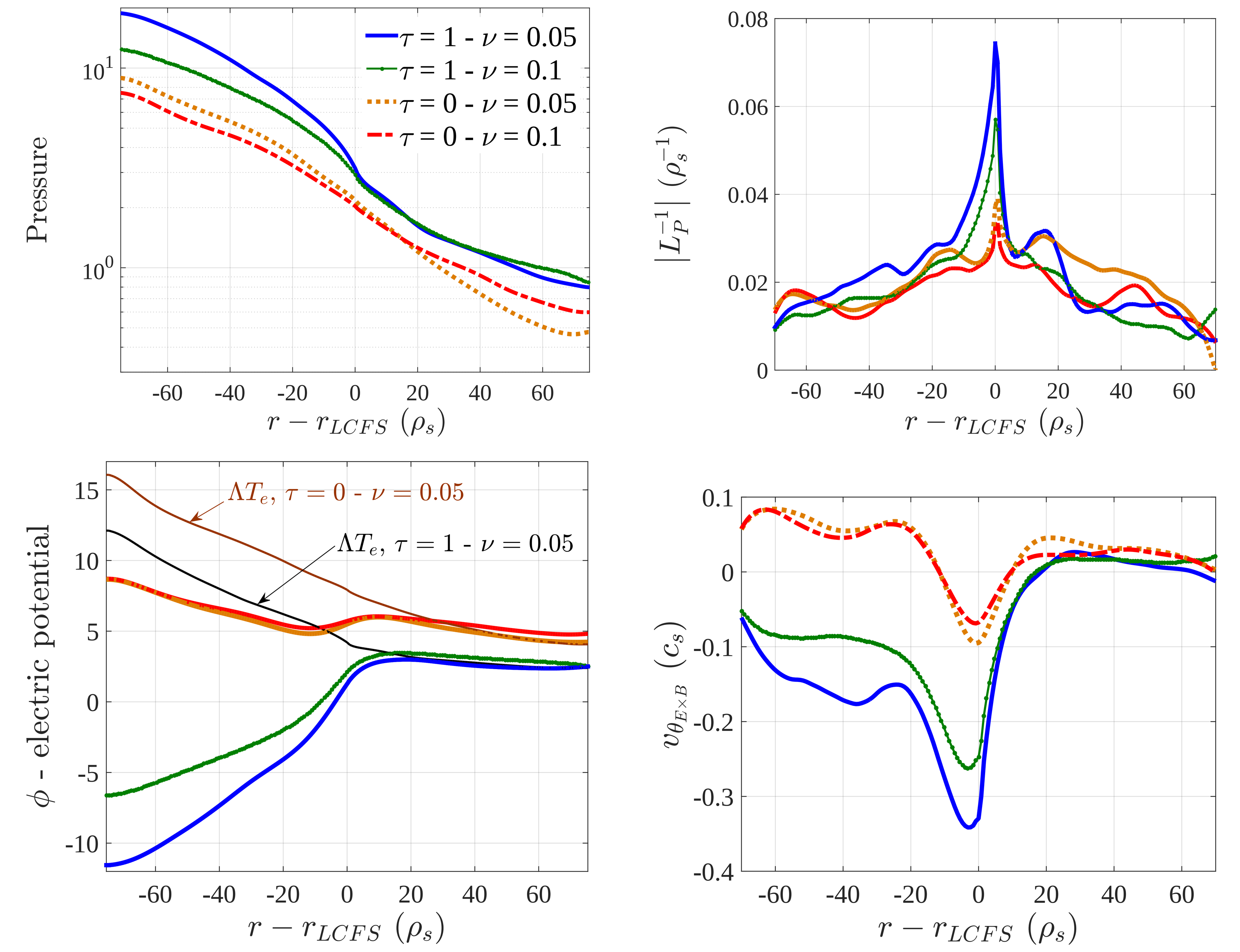

This work has been carried out within the framework of the EUROfusion Consortium and has received funding from the Euratom research and training programme 2014-2018 under grant agreement No 633053.
The views and opinions expressed herein do not necessarily reflect those of the European Commission.